Multifunctional star-shaped polylactic acid implants for use in angioplasty

Selvaraj Nagarajan, M. S. Kiran, John Tsibouklis and Boreddy Siva Rami Reddy

Towards the development of new biomaterials for use in angioplasty, star-shaped polylactic acids have been synthesised and shown to adhere well to living cells, by *in vitro* and *in vivo* experiments, and to hydrolyse over time in a physiologically relevant environment into biocompatible and bioabsorbable entities that are capable of bestowing properties of anticoagulation and angiogenesis to their living host.

Introduction

Cardiovascular disease, one of the leading causes for death worldwide, is often treated by stent implantation. However, the effectiveness of this treatment is impeded by in-stent restenosis (re-narrowing of blood vessels), which affects *ca.* 20% of patients.[1–3]

The metal skeletons of coronary stents provide mechanical stability, but have been associated with inflammation and thrombosis at the implanted site. To overcome this, the metal skeleton of stents is usually coated with biocompatible[4] and biodegradable[5] polymers which may incorporate drug molecules that inhibit thrombus and vascular smooth muscle cell (VSMC) proliferation.

Consequent to the application of the polymeric coating, the surface of the implanted stent is often lipophililic but over time it becomes increasingly hydrophilic due to the increasing presence of polar functionalities as the molecular weight of the biodegradable polymer is reduced and also due to the associated crystalline-to-amorphous transition caused by the plasticising effect of low molecular weight molecules from body fluids.[3–5] The degree of crystallinity of the polymeric matrix may be further affected by the plasticising effect of the incorporated drug molecules.[6–8] The combined effects of plasticisation and increasing hydrophilicity impact upon the therapeutically useful lifetime of the implant. Crystalline phase hydrolysis begins at the surface and propagates layer by layer whereas at the amorphous phase the initiation and propagation of chain scission is random.[5] Since the time dependence of the degradation rate is key to prolonging the release of the drug from the polymer matrix, the physical blending of drug molecules and polymer often results in lower degrees of crystallinity, and consequently accelerated rates of degradation. The drug eluting stents currently in use to overcome in-stent restenosis are often ineffective due to the rapid washout of the drugs from the local delivery sites in the arterial wall.[9] The use of sustained drug eluting stents carries alternative risks such as delayed endothelial regeneration and late thrombosis, which may cause implant rejection. Thus, the current impetus for the considerable research activities towards drug eluting stents is

provided by the need to reduce the incidence of implantation-associated thrombosis. It has been reported that the vessel endothelium plays an important role in preventing thrombosis and hyper- plasia.[7,9] Rapid smooth muscle cell proliferation and delay of re- endothelisation have been found to be the pathophysiological events leading to thrombosis and in-stent restenosis.

The involvement of lactide in biochemical processes renders the ring opening products of this monomer biocompatible and biodegradable materials for a range of biomedical applications,[4,5] including those that require a potent pro-angiogenic effect.[10] Further, the chain length of polylactic acid (PLA), may be readily controlled since the material consists of hydrolysable polyester functional groups and reactive carboxyl/hydroxyl chain-terminating moieties. This in turn affords control over the hydrophilic–lipophilic balance (HLB) of the material.[11] HLB, a determinant parameter of the rate of biodegradation, may be tuned through the appropriate design of star- or comb-shaped molecular structures that allow the interplay between the polyester chain length and the number of terminal functional groups,[12] as illustrated in Fig. 1.

In this work, the well-known drug dipyridamole has been used as a co-initiator with tin(II)ethylhexanoate (Sn(Oct)2) to effect control over the degradation/hydrolysis rate of the resultant polymer and to enhance its capability to inhibit thrombus formation and vasodilation. The molecular design is rationalised by literature observations that if constructed around a dipyridamole core, the resultant star-shaped PLA polymer may combine biocompatibility and controlled biodegradability with the therapeutic benefits (anti-thrombogesis,[13–15] anti-inflammation,[16,17] and compatibility with the extra cellular matrix[18,19]) of the constitutional sub molecular units (Scheme 1). Thus, this paper also provides a preliminary assessment of star-shaped dipyridamole-cored PLA as a coating of coronary stents that may promote angiogenesis-facilitated re-endothelisation and prevent thrombosis and in-stent restenosis.

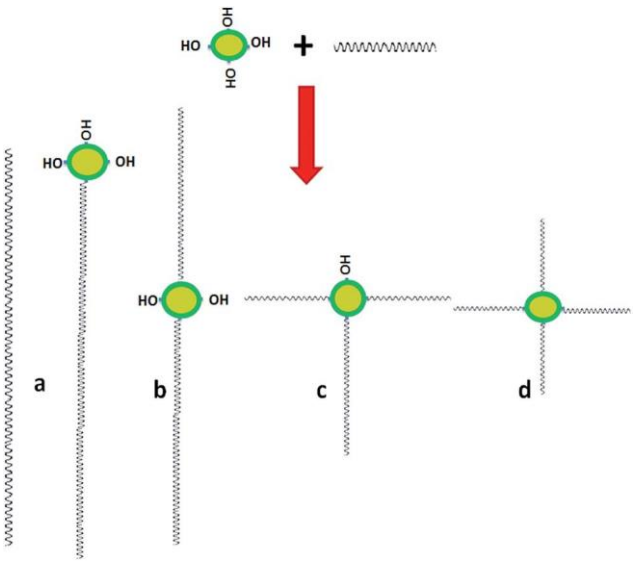

Fig. 1 Effect of molecular shape and structure on hydrophilicity of PLA (a < b < c < d).

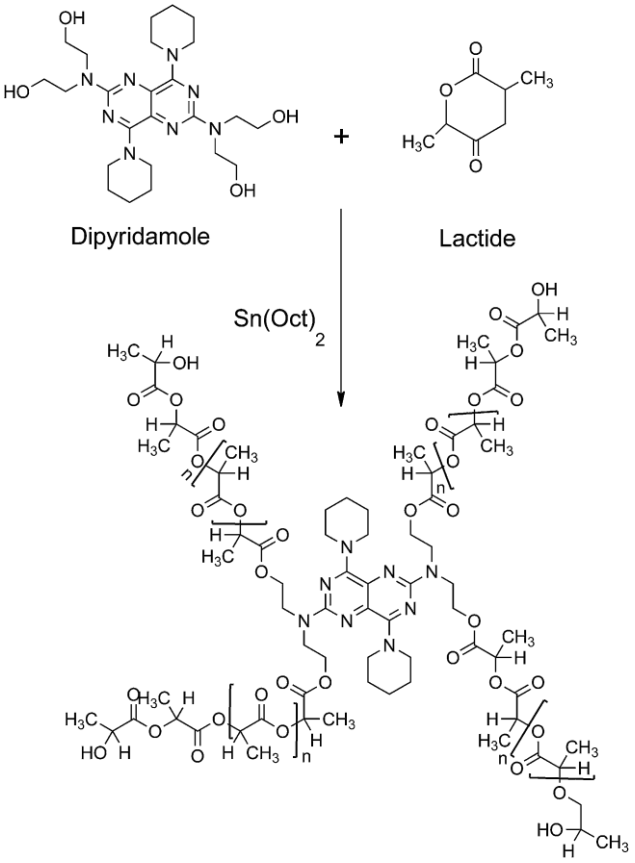

Scheme 1 Synthesis of star-shaped PLA with a dipyridamole molecular core.

Experimental

Materials

Dipyridamole, $_{L}$-lactide, $_{DL}$-lactide, tin(II)ethylhexanoate (Sn(Oct)2), 3-(4,5-dimethylthiazol-2-yl)-2,5-diphenyltetrazolium bromide (MTT), fetal bovine serum (FBS), Dulbecco's Modified Eagle's Medium (DMEM), Minimum Essential Medium Eagle (MEM), haemoglobin reagent, Wright's stain/Leishmann stain, formaldehyde, calcium chloride, $_{D}$-glucose, sodium citrate and citric acid were obtained from Sigma Aldrich. Phosphate buffer saline was sourced from Hi-media. Chloroform, hexane, ethanol, methanol and sulfuric acid were purchased from Rankem. All materials were used without further purification. Toluene (Rankem) was dried over a sodium wire.

Instrumentation

^{1}H-NMR spectra (TMS, $CDCl_3$) and ^{13}C-NMR spectra (TMS, $CDCl_3$) were obtained with a Jeol ECA spectrometer operating at 500 MHz and at 125 MHz respectively. Molecular weight distribution profiles were determined by GPC (30 ^{o}C; THF, 1 ml min^{-1}) using a Jasco-MX2080-31 instrument equipped with a mixed-C column and a RI detector. Polymers were injected (50 µl) into the column as solutions in THF (5 mg ml^{-1}); monodisperse polystyrene standards facilitated primary calibration. A TA-Q200 DSC instrument operating at 10 ^{o}C min^{-1} facilitated the study of the thermal behaviour of polymers (5 mg; aluminum pan; nitrogen atmosphere) over the range 0–180 ^{o}C. Polymer films were deposited from solution in chloroform onto glass substrates (22 mm x 22 mm). Contact angle measurements (water, 10 µl; HO-IAD-CAM-01 goniometer, Image J1.36b software) were performed on film structures that had been allowed to dry (room temperature, 24 h) in a dust-free environment.

Synthesis

$_{L}$-Lactide or $_{DL}$-lactide (2 g) was introduced into a round-bottomed flask (100 ml). Dry toluene (25 ml) was added to the vessel (constant stirring; dry nitrogen atmosphere) followed by a specified amount of dipyridamole (7 or 10 mg) in toluene (10 ml). Then $Sn(Oct)_2$ (10 mg) was added and the temperature was allowed to increase to 100 ^{o}C. After heating for 24 h, the cooled reaction mixture was condensed to about half of its original volume (rotary evaporation) and the product was isolated by suction filtration following precipitation from ethanol/hexane (400 ml; 20/80 v/v). The solid product was washed with methanol and dried under reduced pressure.

Hydrolytic weight loss

Hydrolytic weight loss experiments were conducted in vials (2 ml) containing the powdered sample (50 mg) and phosphate buffer solution (PBS; 1 ml). To simulate body temperature and long-term ageing, samples were maintained over specified time scales in a hot air oven at 37 ^{o}C and 70 ^{o}C. Weight loss was determined gravimetrically (±0.1 mg), following isolation (centrifugation, 5000 rpm) and drying (vacuum oven; 24 h, 70 ^{o}C) of the insoluble polymer fraction. Experiments were performed in triplicate and analysed using the Student's *t*-test. Weight loss was expressed as a percentage of the original weight.

Separation of the hydrolysis product of star-shaped PLA

Star-shaped PLA was hydrolysed by placing accurately weighed samples of the material (*ca.* 50 mg) in phosphate buffered saline (PBS, 1 ml) at 70 ^{o}C for 10 days. The supernatant was separated by centrifugation and the extent of hydrolysis was determined as the weight loss from the dried solid mass that remained in the centrifugation vessel. The diluted supernatant at specified concentrations was used for *in vitro* and *in vivo* studies.

MTT toxicity assay

The *in vitro* cell toxicity of the hydrolyzed products (PBS solution) of star-shaped polymers was assessed by means of the MTT assay. Fibroblasts (NIH3T3; 1 x 10^{4} cells per ml) were grown overnight (48-well plate; 37 ^{o}C; 95% air, 5% CO_2) in DMEM containing 10% fetal calf serum (FCS). Following removal of the medium, cells were washed with DMEM containing 10% FCS before incubation (72 h) with specified concentrations of the hydrolysed polymer (0.501 mg ml^{-1}, 1.02 mg ml^{-1}, 2.04 mg ml^{-1}, 4.08 mg ml^{-1} and 8.16 mg ml^{-1}). Controls were provided by cell cultures that had been prepared in the absence of the hydrolysed polymer. Toxicity was assessed at 24 h intervals. Cells were treated with MTT in PBS (0.5 mg ml^{-1}), incubated (CO_2) for 4 h and DMSO was added to solubilise the coloured product formed as a result of the reduction of MTT by viable cells. The amount of coloured product formed is directly proportional to the number of viable cells. The plates were read at 570 nm using a Bio Rad 650 micro plate reader. Percentage inhibition and cell viability are reported relative to those of the corresponding control.

In vitro assessment of blood compatibility

For the *in vitro* evaluation of blood compatibility of SSPLA, the hydrolysis product of PLA polymers (5 ml) was mixed with fresh blood (100 µl) and EDTA (5 mmol l^{-1}). An aliquot (20 µl) of this mixture was added to hemoglobin solution (5 µl) before incubation (15 min, room temperature) and

subsequent evaluation by means of the *cyanmethemoglobin* method (HEMOCOR-D; 540 nm). The changes in the platelet counts were monitored using a Neubauer's chamber.

Platelet preparation and aggregation assay

Blood platelets drawn from healthy volunteers were placed into an anticoagulant solution (0.15% v/v) of acid-citrate-dextrose (ACD: 38 mM citric acid, 75 mM Na citrate, 124 mM dextrose).[20] Platelet-rich plasma was isolated by centrifugation (180*g*; 10 min; room temperature) and then acidified to pH 6.5 with ACD and prostaglandin E1 (1 mM). The platelets were pelleted down by centrifugation (750*g*, 10 min, room temperature), suspended in a mixture of NaCl (130 mM), trisodium citrate (10 mM), $NaHCO_3$ (9 mM), dextrose (96 mM), $MgCl_2$ (0.9 mM), KH_2PO_4 (0.81 mM) and Tris pH 7.4 (10 mM), and then treated with $CaCl_2$ (1.8 mM). Platelet aggregation studies were performed at 3, 6, 9 and 12 min using a microplate (37 ^{O}C; vigorous shaking; optical density measured at 405 nm). At each test concentration, samples of the hydrolysis product of SSPLLA or SSPDLLA in PBS (8 µl) were mixed with aliquots (90 µl) of platelets. Thrombin (0.2 units per ml) and heparin (4 units per ml) were used as positive and negative controls.

Cell adhesion assay

The cell adhesion assay was performed by maintaining (24 h or 48 h) the 3T3-L1-fibroblast cells in culture plates (MEM containing 10% FBS) that had been casted with specified PLA derivatives. A culture well coated with collagen served as a control. After 24 h or 48 h of incubation the culture medium was removed, and followed by washing with PBS, cells were fixed by first adding ethanol (96%, 200 µl; 30 ^{O}C; 10 min) and then crystal violet solution (0.1%, 200 µl; room temperature; 30 min). Excess stain was removed by repeated washing steps with doubly distilled water. Crystal violet associated with cell nuclei was extracted by the addition of Triton-X100 (0.2%, 100 µl) and quantified by absorbance measurements at 570 nm. The reported measurements are means from three experiments.

Isolation and culture of endothelial cells from rat aorta

Rat aorta endothelial cells (RAECs) were isolated from thoracic aortas that had been excised from 3 week-old Sprague-Dawley rats following sacrifice of the animal. Following the removal of the surrounding fibro-adipose tissue (fine dissecting forceps) and after discarding the proximal and distal regions, aortas were cut into 1 mm ring sections and cultured (DMEM containing 10% FCS) in a CO_2 incubator (95% air, 5% CO_2; 37 ^{O}C), according to the procedure of Nicosia *et al.*[21] RAECs were sourced from endothelial sprouts that formed from aortic rings and cultured in DMEM containing 10% FCS. The efficacy of the hydrolysis product of SSPLLA or SSPDLLA to promote angio- genesis was assessed by treating these cells with specified concentrations of each degraded polymer. The angiogenic efficacy was evaluated by comparing (LeicaQWIN software)

tubular network formation [length (μm) of endothelial capillary sprouts] in ECs with those in untreated controls.

Aortic ring assay for angiogenesis

The aortic ring assay[22] was carried out by exposing aortic rings maintained in DMEM containing 10% FCS to the hydrolytic products of star-shaped PLA. To this end, aortic rings were loaded onto a 24 well plate (10 pieces per well) and cultured (CO_2 incubator) in DMEM containing 10% FCS and specified concentrations of the hydrolysis product of SSPLLA or SSPDLLA.

The efficacy of angiogenesis was evaluated photomicro-graphically, by comparing the sprouting in aortic rings with those in controls (prepared following an identical procedure, but in the absence hydrolytic products of star-shaped PLA) at specified time intervals. The medium was replaced after 24 h. The extent of angiogenic response was quantified (area per μm^2) by comparing (Leica QWIN software) the total area and the number of aortic sprouts in samples with those of controls.

All animal experiments were performed as per the animal handling protocol conformed to the international standards, and was monitored by the Institutional Ethics Committee.

Chorioallantoic membrane assay

The chorioallantoic membrane (CAM) assay[23] was performed using white Leghorn eggs collected from the poultry research station in Madhavaram, Chennai. Fertilized eggs were incubated in a humidified incubator (37 ^oC; relative humidity 80%) for four days, after which time the eggs were candled to identify prominent blood vessels and to assess the development of the embryo. A window (1 cm^2) was cut over the CAM (small craft- grinding wheel) and test samples were loaded onto a hydro-cortisone-dried filter disk and placed on the CAM at a vascular area near a previously identified prominent blood vessel. The window was sealed with sterile parafilm and the eggs placed back in the incubator. Changes in microvasculature density were assessed (digital imaging) after four days of incubation.

Results and discussions

^{1}H- and ^{13}C-NMR spectroscopy

Star-shaped PLA polymers were synthesized by a coordination intersection reaction in which the $Sn(Oct)_2$-catalysed polymerization of $_L$-lactide was initiated by the primary tetra-hydroxyl groups of dipyridamole to give a secondary hydroxyl group-terminated, four-armed structure. The ^{1}H-NMR spectrum of SSPLLA is presented in Fig. 2. The stereochemistry of lactide impacted upon the

microstructural order, which in turn influenced the crystalline order and optical activity as shown in Table 1.[24]

^{13}C-NMR spectral data from Fig. 3, allowed the assessment of the Bernoullian probability of tetrad- and hexad-sequence distributions. The ^{13}C-NMR spectra of SSPLLA and SSPDLLA with similar molecular weight and PDI polymers were synthesized for comparing the resonances at 69.00 and 169.69 ppm attributing to CH and COO functionalities. SSPLLA exhibited a single chemical shift for CH at 69.1 ppm and COO at 169.7 ppm representing the tetrad sequence of iii, iis, sii and sis and the hexad sequence of iiiii, iiiis, siiii and siiis. This confirms that SSPLLA exists in a predominantly isotatic microstructure. On the other hand, in the case of SSPDLLA, additional signals for the CH group at the 69.3 ppm (isi) and 69.5 ppm (sss) tetrad sequence were seen. The chemical shift for the hexad sequence of the COO group at 169.15–169.45 ppm (iiisi, iisii, sisii, sisis, iisis and isiii) and 169.05–169.15 ppm (isisi)[25] is consistent with the existence of atactic polymer chain arrangement. This was further supported by optical rotation data for SSPLLA ($[\alpha]_D^{27}$ ¼ -156^o, in chloroform). The formation of optically inactive SSPDLLA is consistent with the random distribution of tetrad and hexad sequences in atactic microstructural arrangements.

Thermal and contact angle behaviour of star-shaped PLA

The effects of tacticity on the thermal properties of star-shaped PLA polymers were studied by DSC, Table 2. Isotactic SSPLLA is semi-crystalline, exhibiting both T_g and melting endotherms, whereas heterotactic SSPDLLA is amorphous. Accordingly,[26,27] the midpoint of the T_g range of heterotactic SSPDLLA was seen at a lower temperature (33 ^{o}C) than that of isotactic SSPLLA (53 ^{o}C), Fig. 4. The DSC data indicated that tacticity influenced the molecular arrangement. Contact angle measurements revealed that the order of hydrophilicity, as determined by water contact angles on films, was PLLA > SSPLLA > SSPDLLA; respective contact angles were measured at 80^o, 68^o and 67^o (Fig. 5). The order of hydrophilicity was further reflected by the rate of hydrolysis, as presented in Fig. 6. Although average molecular weight may be of some significance, it is assumed that the main factor influencing the rate of hydrolysis is the degree of crystallinity, which in turn is influenced by the tacticity of each polymer.[28,29]

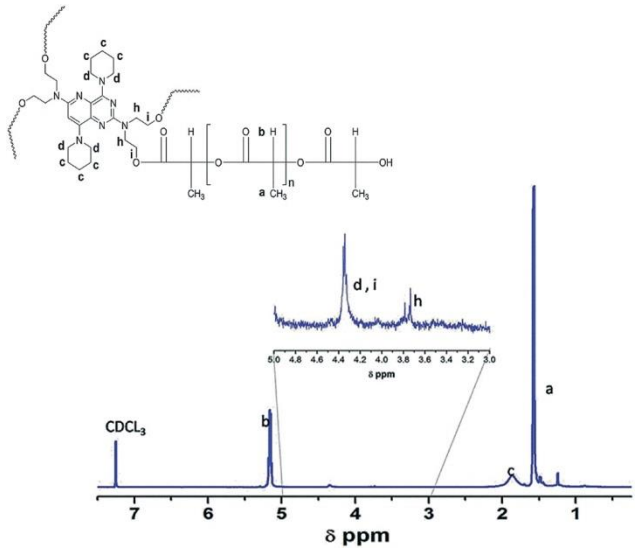

Fig. 2 ^{1}H-NMR spectrum of SSPLLA. H-NMR (500 MHz, CDCl3-d1, d): 1.57 (d, CH3, *J* ¼ 7.55 Hz), 1.65 (s, CH2), 5.2 (q, CH, *J* ¼ 6.87 Hz), 4.3 (q, CH2, *J* ¼ 6.9 Hz), 2.1 (s, CH3), 3.7 (s, CH2).

Table 1 Tetrad and hexad sequence proportions of SSPLLA and SSPDLLA

	Tetrad intensity (%)				Hexad intensity (%)					
Monomer[a]	ssi	sss × 10^{-3}	isi	iss × 10^{-3}	sis, iis, sii, iii	siiii, iiii, iiiis, iiis	iiisi	sisii, isiii, iisii	sisis, iisis	D
L-Lactide	—	—	—	—	0.98	00.98	—	—	—	
D,L-Lactide	—	0.03	0.24	0.04	0.75	21.70	13.4	19.2	27.3	

-156°

0°

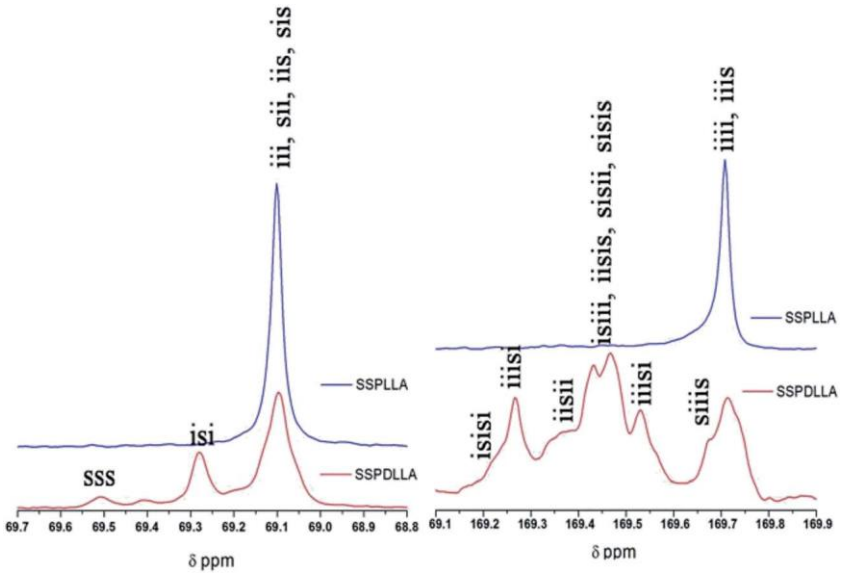

Fig. 3 ^{13}C-NMR of SSPLLA and SSPDLLA fitted with Bernoullian statistical analysis of tetrad and hexad sequence distributions.

Table 2 Molecular weight and thermal behaviour of SSPLLA and SSPDLLA

Composition ratio Lactide (g)										
Entry no.	L	D,L	Dipyridamole (g)	Time (h)	M_n(mol g^{-1})	PDI	T_g (^{o}C)	T_c (^{o}C)	T_m (^{o}C)	DH_g (J g^{-1})
1	2	—	0.010	48	41 500	1.40	53	—	161.24	86.05
2	—	2	0.007	48	32 000	1.35	33	—	—	—

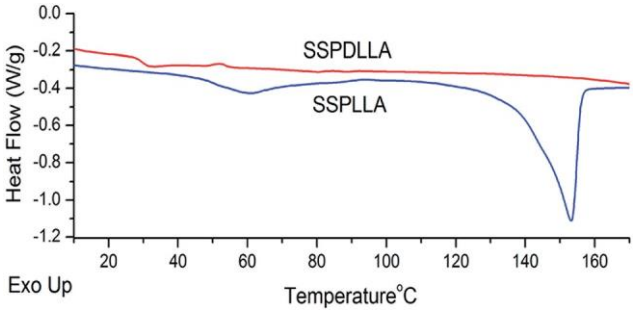

Fig. 4 DSC traces of SSPLLA and SSPDLLA.

Hydrolysis of star-shaped PLA

Hydrolysis weight loss of star shaped polylactic acids with different time periods is shown in Fig. 6. Weight loss of SSPLLA shows a moderate degradation rate with respect to the crystal- line composition and the crystalline packing of the polymer in general (PLLA (isotactic) crystallized in the a-form with 10$_3$ helical conformations).[30–32] In the stereocomplex of $_D$ and $_L$ units, SSPDLLA (heterotactic) crystallized based on hydrogen bonding between the methyl and carbonyl group (CH_3···· O=C). Zange *et al.*[33] reported that the CH_3···· O=C hydrogen bonding leads to the crystallization with 3$_1$ helical conformations in the stereocomplex systems. At the same time, this hydrogen bonding will produce a more amount of amorphous phase in the polymer chain due to the physical cross linking effect.[34–37] So the amorphous phase of SSPDLLA is higher compared to that of SSPLLA. The DSC results in Fig. 3 clearly indicate that the T_g of the SSPDLLA shifted towards lower temperature confirming that the flexibility is more than that of SSPLLA. Here, the higher amorphous phase undergoes random chain scission and the weight loss of the SSPDLLA is more than two folds faster than that of SSPLLA. The hydrolysis rate of SSPLLA follows zero order and first order with the R^2 values of 0.93 and 0.94 respectively in Fig. S2.† But, in the case of SSPDLLA, the R^2 values were found to be 0.78 and 0.73 respectively due to random chain scission. The molecular weight of the SSPDLLA was decreased from 32 000 to 17 664 in Fig. S3.† A clear shoulder was observed on the 4th day during hydrolysis and the fragment of oligomer was found to have a molecular weight of less than 762 g mol^{-1}.

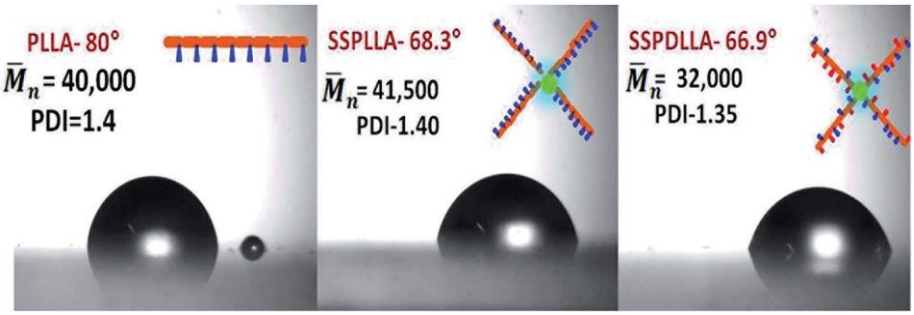

Fig. 5 Contact angle measurement of PLLA, SSPLLA and SSPDLLA in water.

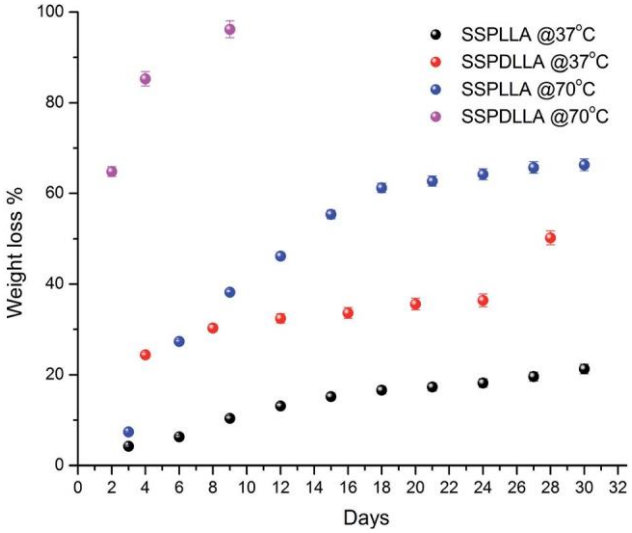

Fig. 6 Hydrolytic degradation profiles for SSPLLA and SSPDLLA in phosphate buffer saline (PBS) solution at 37 ^{o}C and 70 ^{o}C.

Biocompatibility

MTT-assays allowed a preliminary evaluation of the toxicity of the degradation products of SSPLLA and SSPDLLA, Fig. 7. Both degradation products (water soluble fractions with dipyridamole) were seen to cause a significant increase in the proliferation of HaCaT cells relative to the degradation-product-free control. SSPLLA exhibited pronounced effects at several concentrations (0.501 mg ml^{-1}, 1.02 mg ml^{-1}, 2.04 mg ml^{-1}, 4.06 mg ml^{-1}, and 8.16 mg ml^{-1}). Consistent with the hydrolysis of the polymer to its lactic acid precursors, even at 8 mg ml^{-1}, there was no evidence of any toxic effect over 72 h. These results indicate the higher proliferative effect of the degradation product of SSPLLA as compared with that of SSPDLLA. On the basis of literature reports,[38,39] we have concluded that this may be due to the absorption and utilization of the $_{L}$-form of lactate, which is naturally available in humans as opposed to the $_{D}$ and $_{L}$ mixture found in the degradation products of SSPDLLA. The results indicated that the degradation products of the PLA construct are biocompatible and induce cell proliferation.

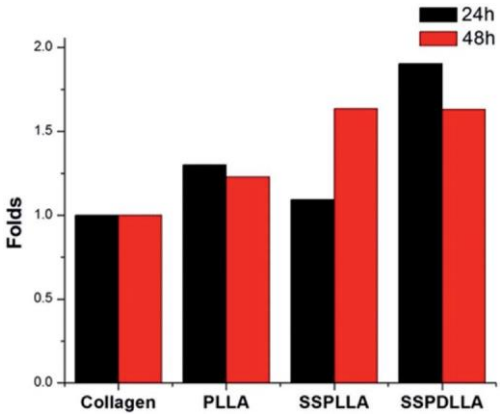

Fig. 8 Effect of collagen, PLLA, SSPLLA, SSDPLLA on NIH 3T3-fibro- blast cell adherence *n* ¼ 3 (24 h and 48 h).

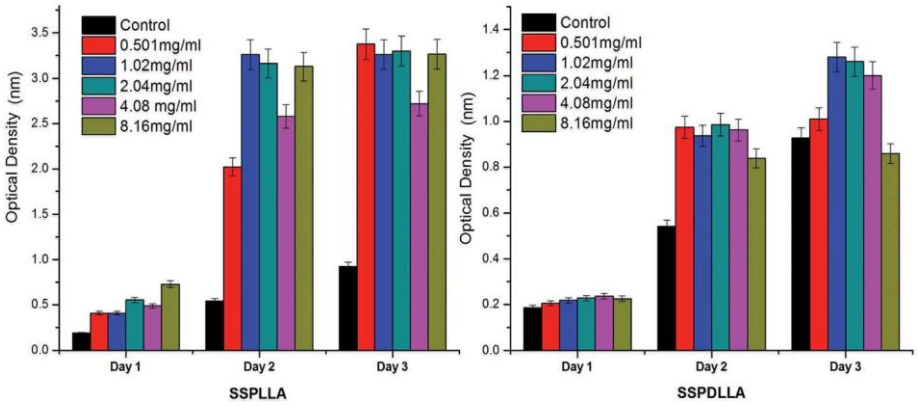

Fig. 7 MTT Assay: effect of SSPLLA and SSPDLLA on cell viability and biocompatibility with concentrations of 0.501 mg ml^{-1}, 1.02 mg ml^{-1}, 2.04 mg ml^{-1}, 4.08 mg ml^{-1} and 8.16 mg ml^{-1}.

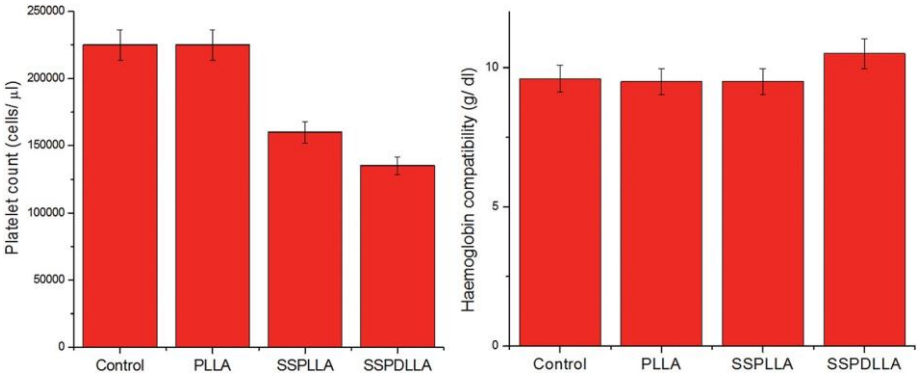

Fig. 9 Effect of control, PLLA, SSPLLA and SSPDLLA on hemocompatibility and platelet count.

Cell adherence

The cell-adherence behaviour of the polymer was compared with the traditional implant materials, collagen and PLLA. The star-shaped polymers exhibited greater affinity for cells as evaluated by the cell adhesion assay, Fig. 8. The SSPDLLA polymer shows maximum cell adherence that is nearly two fold that of collagen, Fig. 8. This may due to the disordered arrangement of polymeric chains leading to the increase in the free volume or the amorphous phase of the material. Crystalline or ordered arrangement of polymeric chains in SSPLLA leads to low free volume and limits cell adherence at the surface of polymeric crystal phases. Accordingly, long and linear chains of PLLA inhibit cell adherence more than star shaped polylactic acid samples. Since there appears to be an inverse relationship polylactic acid chains, and hence free volume, is a determinant factor influencing adhesion to cells.

Blood compatibility of star-shaped PLA

While hemo-compatibility values for SSPLLA and SSPDLLA polymers are comparable with those of the control, the hydro- sylate from PLA polymers causes a reduction in the blood-platelet count, Fig. 9. It is assumed that the reduction is due to the pharmacological effects of the dipyridamole moiety as well as the bio- and hemo-compatible lactides present in the poly- mer. We have observed that cell adhesion is better in $_{D,L}$-lactide oligomers, and that $_{L}$-lactide oligomers exhibited superior blood compatibility. This may be due to the presence of the $_{L}$-form, biological, lactate. To further assess the anti-platelet aggregating effects of PLA polymers, the effect of the hydrolysis products of SSPLLA and SSPDLLA on platelet aggregation was between the degree of crystallinity and the amount of adhered polymer, it was assumed that the rotational freedom of studied, Fig. 10: the expected, platelet anti-aggregating proper-ties were observed. Also, the hydrolysis products of both SSPLLA and SSPDLLA demonstrated a concentration-dependent inhibition of platelet aggregation that was similar to that induced by heparin. These results confirmed the anti-platelet aggregating properties of the constructs, indicating that the construct would prevent the inflammatory response that usually is associated with stent implantation. The prevention of initial neo-intima formation thereby reduces the probability of in-stent restenosis. It is assumed that the anti-platelet aggregation properties of PLA polymers are mainly due to the bio- and hemo-compatibility of lactide rather than that of dipyridamole, which is present at low concentrations. However molecular design considerations necessitated the incorporation of the dipyridamole core as a means of preventing initial platelet activation. Blood compatibility and platelet count studies demonstrated that PLA polymers do not elicit any platelet-aggregating effects.

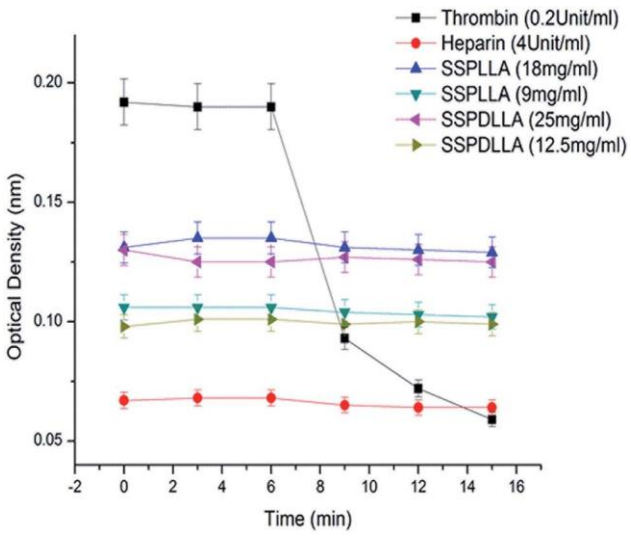

Fig. 10 Effect of the hydrolytic products of star-shaped polylactic acids on platelet aggregation.

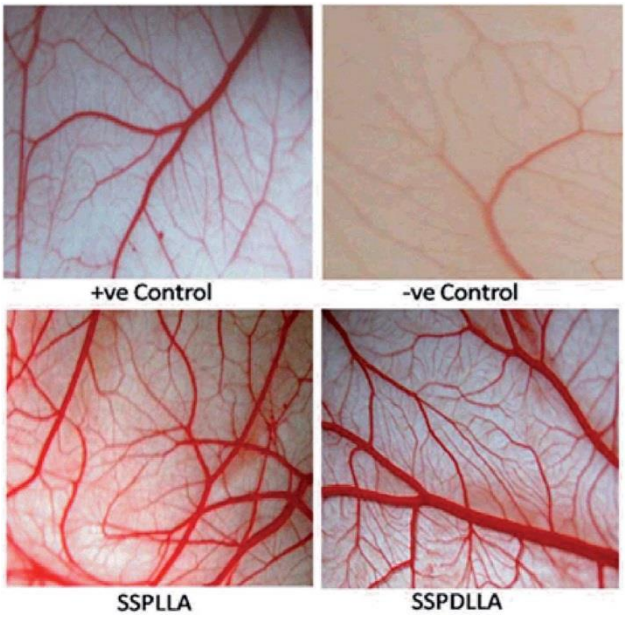

Fig. 11 Effect of SSPLLA and SSPDLLA on *in vivo* angiogenesis: CAM assay with the branching points of 175 and 210.

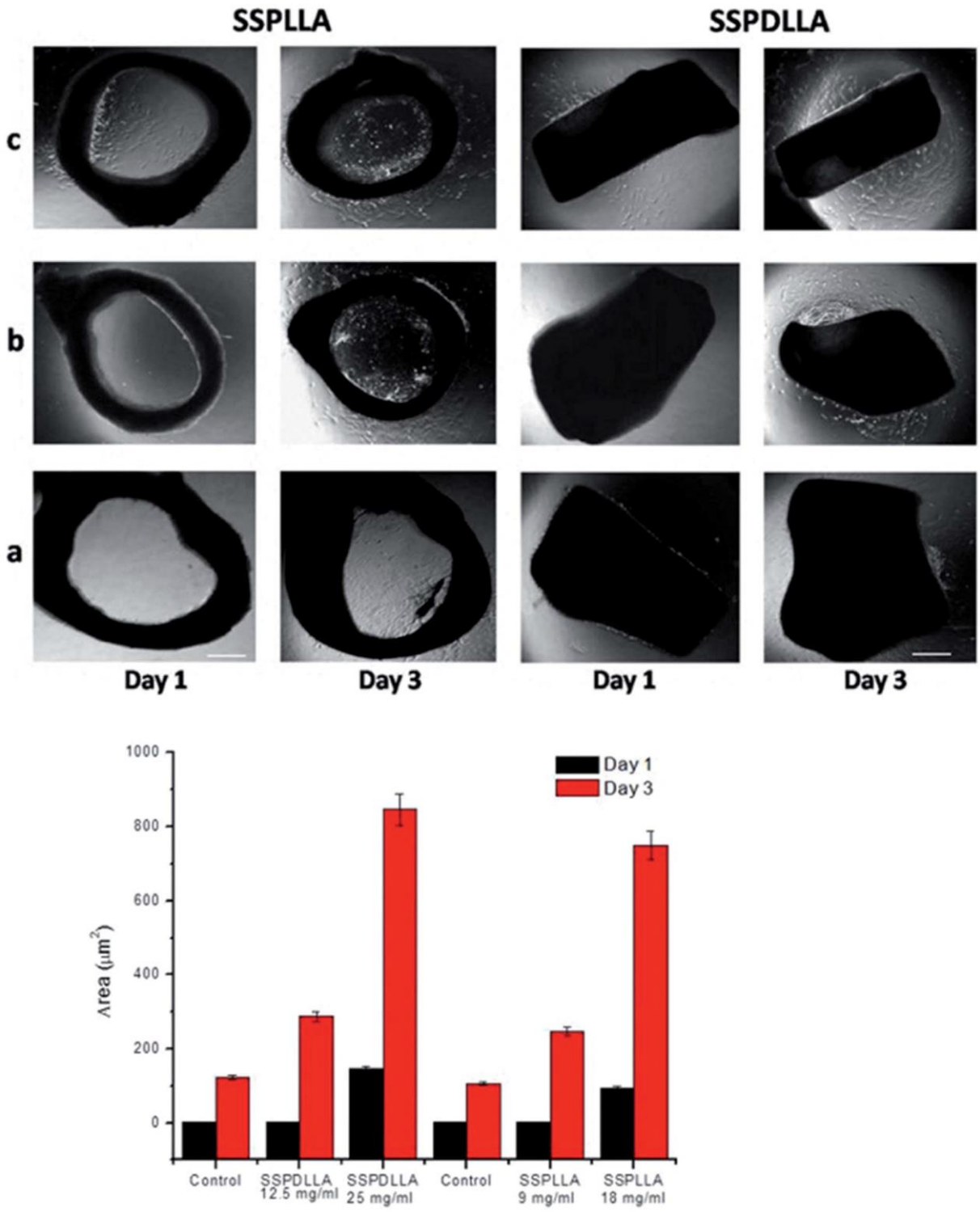

Fig. 12 Effect of SSPLLA, SSPDLLA and control on angiogenesis: aortic ring assays. The scale bar represents 10 μm.

Effect of SSPLLA and SSPDLLA on angiogenesis

CAM assay. The CAM assay demonstrated that treatment with SSPLLA or SSPDLLA causes a significant increase in the mean diameter and in the density of microcapillaries (Fig. 11) as

compared with both the positive (endothelial growth factor) and negative (endostatin) controls. The efficacy of SSPDLLA to induce angiogenesis in CAM was greater than that of SSPLLA. This is attributed to the amorphous nature of SSPDLLA, compared with SSPLLA, allowing more rapid degradation and releasing increased levels of hydrolysed lactates. This in turn results in increased branching in SSPDLLA-(210 branch points) as compared with SSPLLA-(175 branch points). The degradation rate of SSPDLLA is faster than that of SSPLLA, with the implication that the higher availability of the products of the hydrolysis promotes angiogenesis in the CAM assay. This is further supported by the observation that respective branch points in positive and negative controls were 170 and 45; vascular endothelial growth factor-treated CAM provided the positive control and endostatin-treated CAM was used as the negative control. The increased angiogenic efficacy of the polymer as compared with VEGF may be due to lactide which promotes VEGF production and simultaneously inhibits post- translational modification; namely, the polyADP ribosylation of VEGF increasing biological activity.[10] Since the more rapidly hydrolysable SSPDLLA exhibited the highest angiogenic efficacy, it is assumed that angiogenicity is directly linked to the formation of lactic acid during the degradation process. The effect of the hydrolysis product of PLLA and PDLLA on angio- genesis is presented as ESI.† The results indicated that the rate of the proangiogenic effect is in the order: $_{L}$-lactate < $_{D,L}$-lactate < PDLLA < PLLA. Since PDLLA is more readily amenable to biochemical hydrolysis than PLLA, the former material is more proangiogenic. Also, the naturally available $_{L}$ lactate is more proangiogenic than $_{D}$ lactate.

Aortic ring assay. The effect of SSPLLA and SSPDLLA on cell types that are known to be involved in angiogenesis (endothelial cell, fibroblast cells and smooth muscle cells) was assessed by means of an established *in vitro* tissue explant assay, namely the aortic ring angiogenesis assay. The pro-angiogenic effects of SSPDLLA and SSPLLA on aortic rings, as indicated by the length and number of aortic sprouts from explants relative to those for the control, are shown in Fig. 12. Consistent with the CAM assay, the density of aortic ring sprouts that had formed consequent to treatment with SSPDLLA was higher than that induced by SSPLLA. The difference in the rate of angiogenesis in SSPDLLA and SSPLLA may be attributed to the physical nature that dictates the rate of degradation and availability of lactate in the microenvironment to promote angiogenesis.

Effect of SSPLLA and SDPLLA on RAEC differentiation. Consideration of the rate of differentiation of RAECs from a cobblestone morphology to a capillary network-like structure demonstrated a concentration-dependent proangiogenic effect for SSPLLA and SSPDLLA as shown in Fig. 13. In accordance with expectations, the angiogenic efficacy of SSPDLLA was greater than that of SSPLLA.

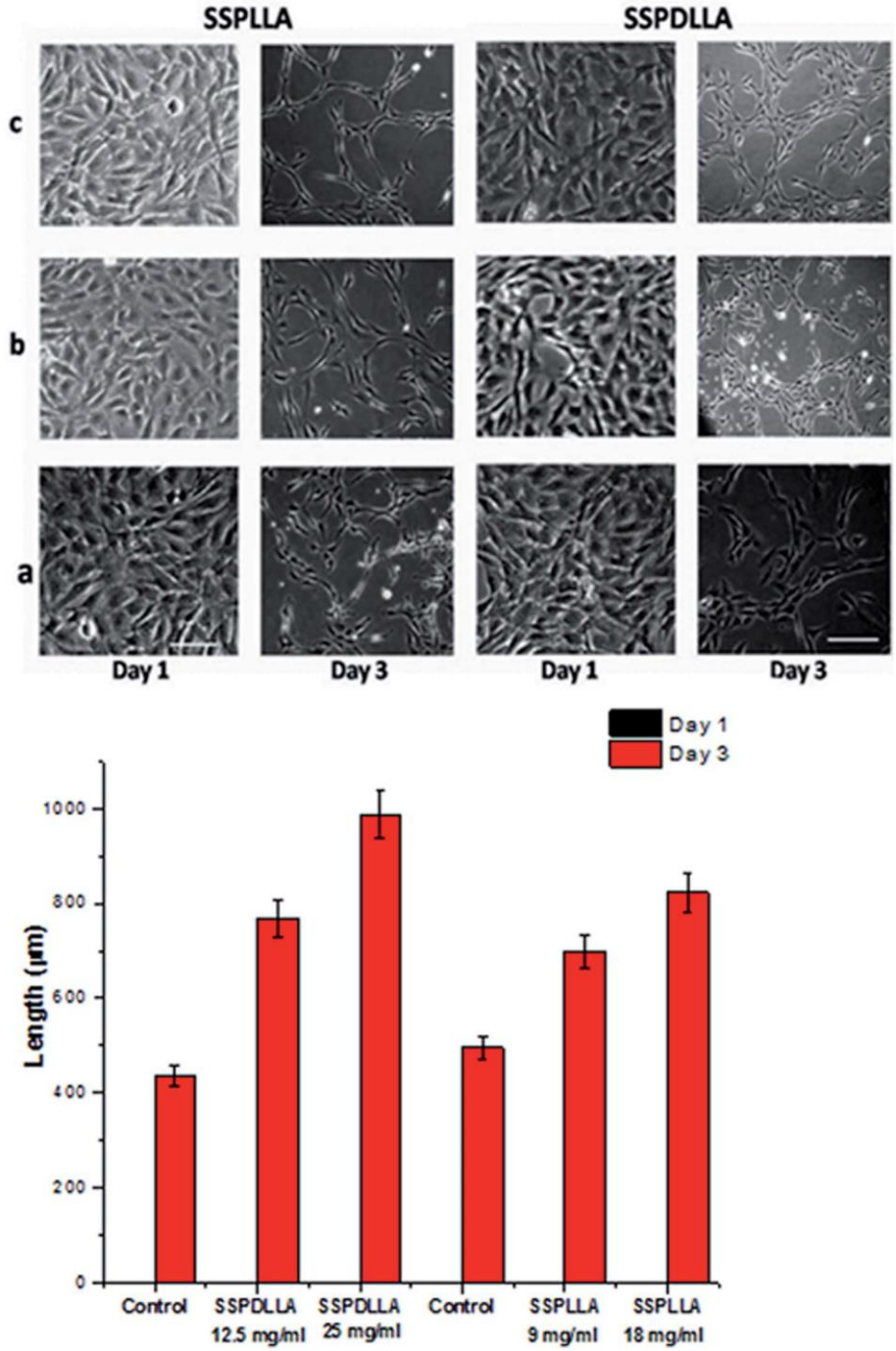

Fig. 13 Effect of SSPLLA, SSPDLLA and control on RAEC differentiation. The scale bar represents 10 μm.

Conclusions

Two star-shaped polylactic acids of differing hydrophilicities have been synthesized and characterised by spectroscopic and analytical techniques. The tacticity of these polymers was found to determine the degree of crystallinity, which in turn was seen to determine hydrolytic stability. A series of *in vitro* and *in vivo* experiments have demonstrated that both polymers combine biocompatibility with properties of anti-coagulation and angiogenesis. These properties render the materials suitable candidates for use in coronary stents for the treatment of cardiovascular disease.

Conflict of interest

Authors declare that there is no conflict of interest.

Acknowledgements

The authors acknowledge financial support from the DST, New Delhi (no. SR/S1/PC-45/2011).

Notes and references

1. Y. Wei, Y. Ji, L. L. Xiao, Q. K. Lin, J. P. Xu, K. F. Ren and J. Ji, *Biomaterials*, 2013, 34, 2588–2599.
2. C. A. Kavanagh, Y. A. Rochev, W. M. Gallagher, K. A. Dawson and A. K. Keenan, *Pharmacol. Ther.*, 2004, 102, 1–5.
3. H. M. Burt and W. L. Hunter, *Adv. Drug Delivery Rev.*, 2006, 58, 350–357.
4. D. Grafahrend, K. H. Heffels, M. V. Beer, P. Gasteier, M. Moller and G. Boehm, *Nat. Mater.*, 2011, 10(1), 67–73.
5. S. Nagarajan and B. S. R. Reddy, *J. Sci. Ind. Res.*, 2009, 68, 993–1001.
6. S. Nagarajan, B. S. R. Reddy and J. Tsibouklis, *J. Biomed. Mater. Res., Part A*, 2011, 99, 410–417.
7. G. Gaucher, M. H. Dufresne, V. P. Sant, N. Kang, D. Maysinger and J. C. Leroux, *J. Controlled Release*, 2005, 109, 169–188.
8. M. Vert, *Biomacromolecules*, 2005, 6, 538–546.
9. J. F. Mitchel, D. B. Fram, D. F. Palme, R. Foster, J. A. Hirst, M. A. Azrin, L. M. Bow, A. M. Eldin, D. D. Waters and R. G. McKay, *Circulation*, 1995, 91(3), 785–793.
10. V. B. Kumar, R. I. Viji, M. S. Kiran and P. R. Sudhakaran, *J. Cell. Physiol.*, 2007, 211(2), 477–485.
11. S. Vrignaud, J. P. Benoit and P. Saulnier, *Biomaterials*, 2011, 32(33), 8593–8604.
12. M. P. Shaver and D. J. A. Cameron, *Biomacromolecules*, 2010, 11(12), 3673–3679.
13. R. Langer, *Science*, 1990, 249, 1527–1533.
14. Y. Wei, Y. Ji, L. L. Xiao, Q. Lin, J. Xu, K. F. Ren and J. Ji, *Biomaterials*, 2013, 34(11), 2588–2599.
15. J. F. Mitchel, D. B. Fram, D. F. Palme, R. Foster, J. A. Hirst and M. A. Azrin, *Circulation*, 1995, 91(3), 785–793.
16. A. M. Lincoff, J. G. Furst, S. G. Ellis, R. J. Tuch and E. J. Topol, *J. Am. Coll. Cardiol.*, 1997, 29(4), 808–816.
17. P. W. Serruys, M. J. Kutryk and A. T. Ong, *N. Engl. J. Med.*, 2006, 354(5), 483–495.
18. M. B. Leon and J. W. Moses, *Adv. Studies Med.*, 2003, 3, S592– S601.
19. J. Taipale and J. Keski-Oja, *FASEB J.*, 1997, 11(1), 51–59.
20. S. M. Anderson, S. N. Siegman and T. Segura, *Biomaterials*, 2011, 32(30), 7432–7443.
21. R. F. Nicosia and G. P. Tuszynski, *J. Cell Biol.*, 1994, 124(1), 183–193.

22. R. F. Nicosia and A. Ottinetti, *Lab. Invest.*, 1990, 63(1), 115–122.
23. K. Z. Olfa, L. Jose, D. Salma, B. Amine, S. A. Najet and A. Nicolas, *Lab. Invest.*, 2005, 85(12), 1507–1516.
24. M. P. Shaver and D. J. Cameron, *Biomacromolecules*, 2010, 11(12), 3673–3679.
25. N. Spassky, M. Wisniewski, C. Pluta and A. L. Borgne, *Macromol. Chem. Phys.*, 1996, 197(9), 2627–2637.
26. J. F. Mano, J. L. GomezRibelles, N. M. Alves and M. S. Sanchez, *Polymer*, 2005, 46(19), 8258–8265.
27. J. Zhang, K. Tashiro, H. Tsuji and A. J. Domb, *Macromolecules*, 2008, 41(4), 1352–1357.
28. X. H. Zong, Z. G. Wang, B. S. Hsiao, B. Chu, J. J. Zhou and D. D. Jamiolkowski, *Macromolecules*, 1999, 32(24), 8107– 8114.
29. N. Cohen-Arazi, A. J. Domb and J. Katzhendler, *Polymers*, 2010, 2, 418–439.
30. K. Aou and S. L. Hsu, *Macromolecules*, 2006, 39, 3337–3344.
31. K. Wasanasuk, K. Tashiro, M. Hanesaka, T. Ohhara, K. Kurihara, R. Kuroki, T. Tamada, T. Ozeki and T. Kanamoto, *Macromolecules*, 2011, 44, 6441–6452.
32. K. Wasanasuk and K. Tashiro, *Macromolecules*, 2012, 45, 7019–7026.
33. J. Zhang, H. Sato, H. Tsuji, I. Noda and Y. Ozaki, *Macromolecules*, 2005, 38, 1822–1828.
34. S. Nurkhamidah, E. M. Woo and K. Tashiro, *Macromolecules*, 2012, 45, 7313–7316.
35. J. Shao, J. Sun, X. Bian, Y. Cui, Y. Zhou, G. Li and X. Chen, *Macromolecules*, 2013, 46, 6963–6971.
36. X. F. Wei, R. Y. Bao, Z. Q. Cao, W. Yang, B. H. Xie and M. B. Yang, *Macromolecules*, 2014, 47, 1439–1448.
37. P. Purnama and S. H. Kim, *Macromolecules*, 2010, 43, 1137–1142.
38. R. Marti, E. Varela, R. M. Segura, J. Alegre, J. M. Surinach and C. Pascual, *Clin. Chem.*, 1997, 43(6), 1010–1015.
39. B. Ling, F. Peng, J. Alcorn, K. Lohmann, B. Bandy and G. A. Zello, *Nutr. Metab.*, 2012, 9, 6.